Modeling Structure and Physiology from MRI Data: How to See the Invisible

Valerij G. Kiselev
Medical Physics, University Medical Center Freiburg

1 The challenge of probing tissue structure

A large number of the presentations at this meeting are about boosting the spatial resolution of MRI. While there are several innovative approaches being pursued, these developments do not promise an image resolution better than of the order of a millimeter when considering MRI of large parts of the human body. This millimeter scale is three orders of magnitude coarser than the fundamental scale of biology – the micrometer size of living cells. Obtaining information on a cellular scale poses a fundamental challenge to future MRI developments in the assessment of normal development, disease etiology, and diagnostic procedures.

An approach with potential to respond to this challenge has already emerged within MRI. As will be described in this lecture, the key idea is to engage biophysical modeling of the MRI signal in terms of microscopic tissue properties, such as cellular and microvascular architectures, differences in magnetic properties among tissue compartments, *etc.* Targeted measurements designed according to biophysical theory can reveal several such (structural and functional) properties using the available image resolution. An illustration of this approach is provided by an MRI modality called vessel size imaging for evaluation of the mean caliber of microvessels (*ca.* 10 micrometer in the normal brain) using MRI at a spatial resolution of about 2 mm.

In general, quantification of tissue microstructure proceeds in two steps. The first step is to develop a forward model that predicts the intravoxel-averaged MRI signal given the tissue microstructure and to collect MRI signals in agreement with theoretical requirements. The second step is to use the developed theoretical framework to address the much harder inverse problem of quantifying characteristics of the biologically relevant subvoxel tissue structure. This "super-resolution" paradigm is applicable mainly to MRI measurements of diffusion and relaxation. The principles of such measurements are explained in this presentation. We begin with delineation of three length scales that contribute differently in the formation of the MRI signal.

2 The three fundamental length/time scales of MRI

Figure 1 illustrates the three length/time scales that are relevant for the formation of the MRI signal [1]. The deepest one is the molecular length scale of MR visible (active) nuclei, angstrom to nanometer. Beyond the intrinsic magnetic and spin (angular momentum) properties of these nuclei, the signal from a population of like spins (*e.g.*, the ^{1}H spins of water) depends on the structure of the host molecule and its motion (*e.g.*, rotation, translation, *etc.*). This motion is typically stochastic and directionally random (isotropic) and, thus, would be extremely complicated to model in detail. However, a great simplification comes from the fact that this molecular motion is extremely fast.

Proc. Intl. Soc. Mag. Reson. Med. 22 (2014)

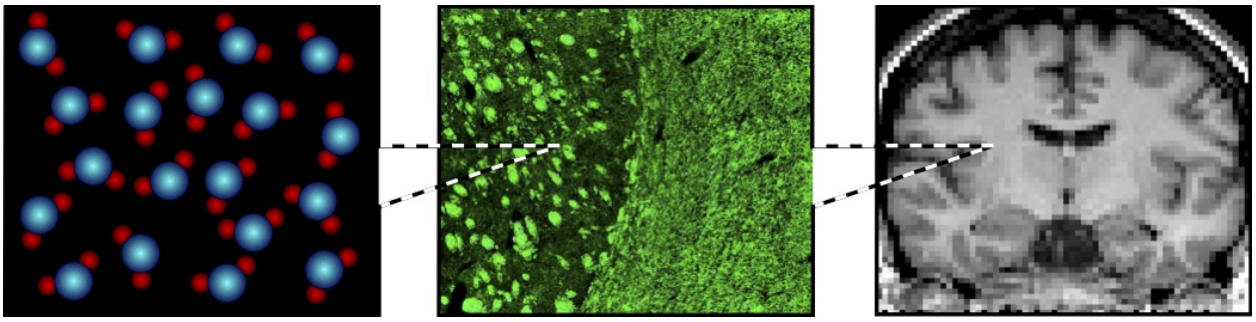

Figure 1: Left: The MRI signal originates from nuclear spin being determined by their interactions and molecular motion. Right: The macroscopic scale of imaging on the order of a millimeter (the image resolution). Middle: The mesoscopic (intermediate) scale of biological cells defining the structure and function of living tissue.

The typical correlation time (memory time) of molecular motion for small molecules (*e.g.*, H_2O) is about one picosecond (10^{-12} sec), which is vastly shorter than the typical time scale of our MR measurements, about one to hundred milliseconds. This, in particular, explains why any attempt to refocus the molecular-motion-perturbed spin phases in such MR measurements is hopeless, since the spin phase history is already forgotten after some picoseconds and any acquired dephasing becomes irreversible. This large separation of time scales (pico- *vs.* milliseconds) results in efficient averaging of molecular-scale (*i.e.*, angstrom to nanometer) spin motion for any kind of MRS and MRI measurements. Detailed information about molecular motion gets lost in this averaging and the only remaining MRI relevant parameters are primarily chemical shifts, scalar coupling constants, spin-lattice and spin-spin relaxation rate constants ($R_1 = 1/T_1$ and $R_2 = 1/T_2$), and the diffusion coefficient. All of these fundamental MR parameters depend on the local chemical composition of the signal-contributing molecules.

Opposed to the molecular scale is the macroscopic scale of imaging, which ranges from the voxel size (millimeter) to the body dimensions (meter). Molecular-diffusion-driven displacement during MRI measurement is negligible on this scale. However, the magnetic fields induced by the magnetic susceptibilities of the large-scale structures of the investigated subject do affect imaging. Since the spatial extents of such susceptibility-induced fields are macroscopic, each molecule is exposed to a practically constant field, whose dephasing effects can be completely refocused using any kind of spin echo.

The above two length scales are the only ones present in classical NMR spectroscopy measurements, which generally are concerned with homogeneous solutions. Tissue biology adds one more length scale, the scale of cells that define the functional and structural role of a given tissue. Molecules of water and other substances diffuse within the highly heterogeneous and tortuous cellular environments. Fortunately, the diffusion-displacement-length during the time available after a single signal excitation is commensurate with the cell size. This means that diffusing molecules do explore the local cellular microstructure.

Beyond the diffusion itself, this structure includes heterogeneous magnetic fields induced by the differing magnetic susceptibilities of cellular compartments; known contributors to this effect are deoxyhemoglobin, myelin, blood doped with a paramagnetic contrast agent, *etc.* The evolution of of spin phase in the presence of such fields is a random process due to the randomness of diffusion

motion. The correlation times (memory times) of such perturbations in spin phase are on the order of one to one-hundred milliseconds, which are commensurate with the timing of MRI measurements. As a consequence, contributions of such motions to transverse ("spin-spin") relaxation cannot be categorized as purely reversible or irreversible dephasing. In general, the processes that are faster than our measurement sequence are irreversible while those that are slower are reversible with all intermediate cases present in biological tissues. This open a possibility to detect the time scales of spin dephasing by varying the type and timing of the measurement sequence. These time scales can be reformulated as structural scales by accounting for diffusion displacement length (and character). This explains why transverse relaxation can act as a probe of tissue structure.

We call the cellular scale mesoscopic to underline its intermediate ("meso") position between the molecular and macroscopic scales. This name is rooted in the notion of mesoscopic physics, a part of condensed matter physics that forms the basis of modern transport theory, and that has enjoyed considerable development over past half a century in the context of transport in semiconductors and other complex materials and media. A synonymous name often used in our MRI community is "microscopic structure" or "microstructure" based on the micrometer scale involved. The rest of this syllabus presents the main MRI modalities suitable for exploring the mesoscopic scale (length/time) of biological tissues.

3 Diffusion MRI

As mentioned above, it is a fortunate fact that the displacement of diffusing molecules during the population lifetime of spin coherence that leads to an observable NMR signal is commensurate with the cell dimensions. The cellular structure is thus reflected in measurable characteristics of diffusion, for example in the time-dependent diffusion coefficient [2, 3]. The challenge is to interpret diffusion measures in terms of the cellular structure(s). A similar challenge is well known in condensed matter physics and there is no simple solution. The first question to answer is what structural properties are still detectable in diffusion metrics after the massive intravoxel-averaging that inevitably occurs due to the macroscopic image resolution (millimeter scale). Indeed, different sub-voxel-populations of molecules report about different local constellations of cells in their contributions to the total signal from a given voxel; all these signal contributions are averaged over the total content of a given imaging voxel (containing millions of cells). Answers to this question can be rather surprising, as illustrated in Fig. 2. In spite of this problem, diffusion MRI is considered today as the main method for exploration of the microstructural architecture of cellular tissue [4].

An example of another insight in the cellular structure is determination of axonal caliber in excised nerves [5] and *in vivo* [6] (Fig. 3). The method is based on theoretical analysis of diffusion in cylindrical compartments associated with axons and then fitting expressions so derived (mathematical form(s) of the biophysical model) to experimental data. The method works well in small-animal scanners equipped with magnetic field gradient assemblies that produce very strong gradients with very short rise times. However, development towards such measurements in human subjects is problematic due to the markedly lower gradient performance (weaker gradients and longer rise times) of clinical scanners.

There is a case in which interpretation of the diffusion-weighted signal is relatively straightforward. It has long been observed that diffusion is highly anisotropic (strong directional preference)

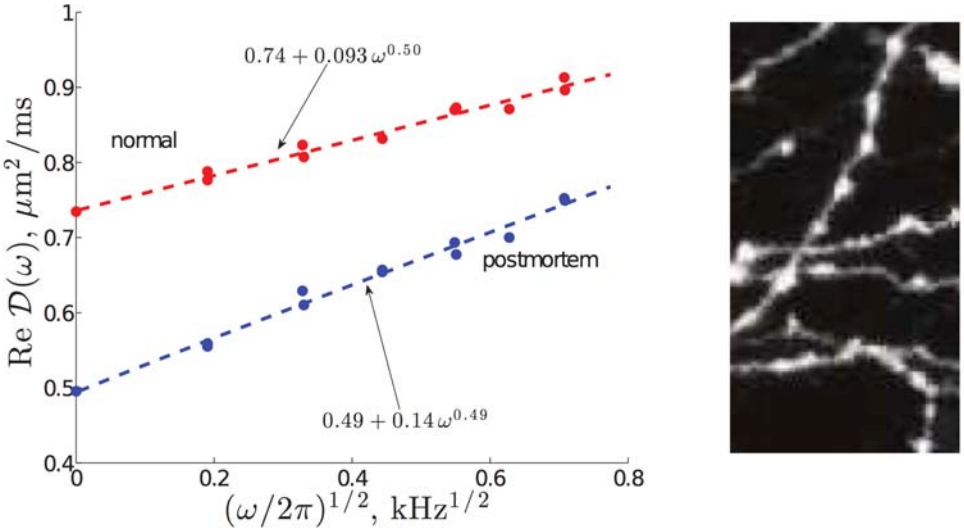

Figure 2: Left: Diffusion coefficient measured in a rat brain using oscillating diffusion-weighting gradients shows a very pronounced frequency (or time) dependence, indicative of the mesoscopic structure [7]. Here we show these data replotted as a function of the square root of oscillation frequency $\omega/(2\pi)$ [3]. Recent theory developed in Ref. [3] predicts a proportionality $\mathcal{D}(\omega) = a + b\,\omega^{\vartheta}$ for different types of structural randomness and spatial dimensionality. In particular, $\vartheta = 1/2$ if diffusion is effectively one-dimensional and is further hindered by randomly placed (uncorrelated) restrictions, such as neurite beads in the right panel. Two-dimensional hindered diffusion (for example in thin sheets) would result in $\vartheta = 1$ and three-dimensional hindered diffusion would result in $\vartheta = 3/2$. Experimental data reveal the predominantly one-dimensional nature of hindered diffusion. As suggested in Ref. [3], this could occur due to the signal primarily originating from within densely packed narrow neurites (dendrites and axons) in brain gray matter (the right panel), which is consistent with well over 50% of volume contained within the neurites as reported using electron microscopy measurements in Ref. [8].

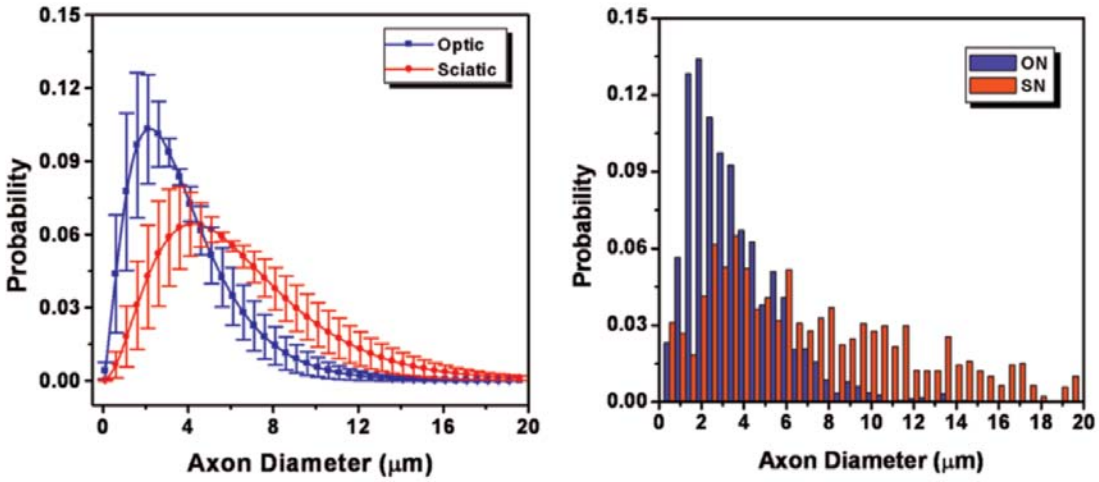

Figure 3: Left: Axon diameter distribution obtained in excised porcine optic and sciatic nerves. Theoretical expressions were combined to describe a gamma distribution of axonal caliber and the result was fitted to experimental data to determine the distribution parameters. Right: Distribution of axonal diameters measured using electron microscopy. Images are reproduced from Ref. [5].

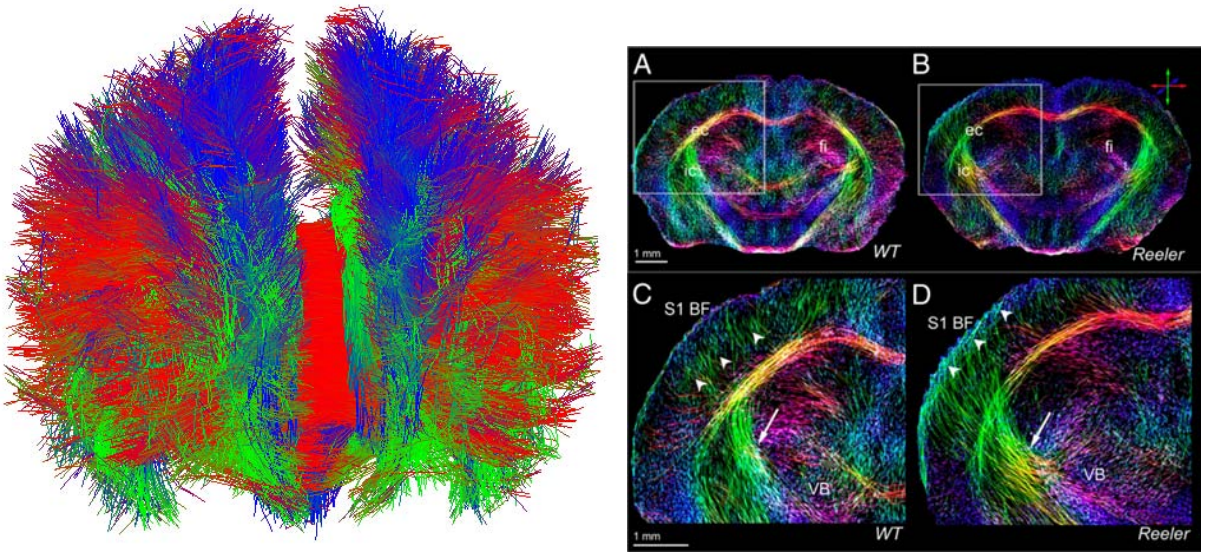

Figure 4: Left: Fiber tracking results in the whole brain [9]. Reconstructed neuronal fibers are represented by lines colored according to their local orientation in space. For analysis, individual fiber bundles are selected by assigning regions they should cross, connect or avoid. Right: Fiber tracking in the mouse brain reveals a re-organization of neuronal fibers in mutant mice with inverse cortical lamination (Reeler). Normal mouse brain (WT) is shown for comparison. Data from Ref. [10].

in brain white matter due to its fibrous structure formed by bundles of axons that connect different parts of the brain and the brain to the body. The diffusion coefficient in the direction parallel to the fibers is significantly higher than in the orthogonal direction. The diffusion anisotropy can thus be interpreted in terms of the local fiber orientation and MRI diffusion data analyzed in terms of the global configuration of neuronal fibers in each voxel, a procedure that is called the fiber tracking. An illustrative result is shown in Fig. 4. One should not be mislead by the simplicity of anisotropy interpretation. An attempt to obtain more detailed information, for example to evaluate structural parameters characterizing the neuronal fibers, faces the same challenge of a deep theoretical development.

4 Transverse Relaxation

Interpretation of transverse relaxation in terms of tissue structure is important for perfusion measurements in the brain using exogenous, paramagnetic, contrast agents, (DSC MRI) [11, 12]. The central problem is to relate the measurable enhancement of transverse relaxation to the concentration of contrast agent in the blood pool; the latter is necessary for evaluation of local tissue perfusion. A closely related technique is the above mentioned vessel size imaging [13, 14, 15]. It is based on a different vessel size dependence of the contrast-agent-induced transverse relaxation measured by gradient echo *vs.* that measured by spin echo as illustrated in Fig. 5.

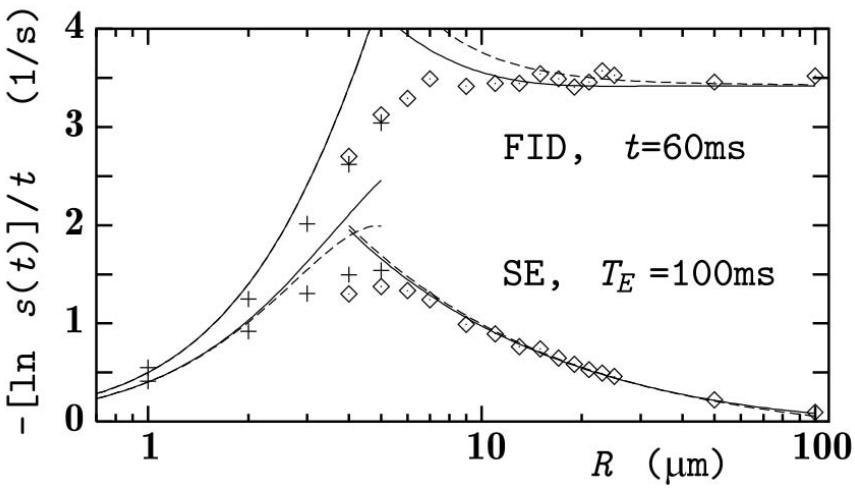

Figure 5: Transverse relaxation rate in extravascular space induced by the presence of paramagnetic contrast in the blood pool as a function of vessel radius of a simulated monosized microvasculature. The dependence is shown for two measurement techniques: Free induction decay (FID), which is measurable using gradient echo sequences, and Hahn spin echo (SE). Symbols show results of Monte Carlo simulations [16] (crosses for permeable capillaries and diamonds for impermeable vessels). Lines present known analytical expressions for limiting cases [17, 18, 19]. Small vessels act as on the molecular scale: the two relaxation rates are close, which indicate an almost irreversible dephasing. Large vessels act as a macroscopic structure: dephasing is observable with the gradient echo is removed by the spin echo. Real capillaries (radius about 3–4 μm) are in the middle with the dephasing intermediate between the above limiting cases. The central idea of vessel size imaging is to measure both relaxation rates and find out the mean capillary size by comparison with theory.

5 Chemical exchange

Chemical exchange refers to the process in which subpopulations of MR-visible nuclei with different, distinct, MR-measurable properties exchange identities. For example, protons (^{1}H) can exchange between water and proteins. All MR-relevant parameters are affected in this case: the chemical shift, the relaxation rate constants, and diffusion properties. Chemical exchange models were originally developed for molecular processes for which the central assumption that all nuclei have equal probability to undergo exchange at any time is well justified (the "well mixed" assumption). Subsequently these models were used and often abused in the context of mesoscopic structure due to their simplicity, which is often misleading. The problem is that chemical exchange models neglect the presence of mesoscopic structure. As was shown in Ref. [20], chemical exchange models can, in principle, be adopted for mesoscopic structure, but are only valid in the long-time limit, when local "short time scale" effects are averaged and all spins identified with a given "compartment" report the same averaged environment ("extreme narrowing" condition).

6 Longitudinal relaxation

True spin-lattice (longitudinal) relaxation (reestablishment of Boltzmann spin-state populations) is determined by molecular interactions that occur over the angstrom length scale as modulated

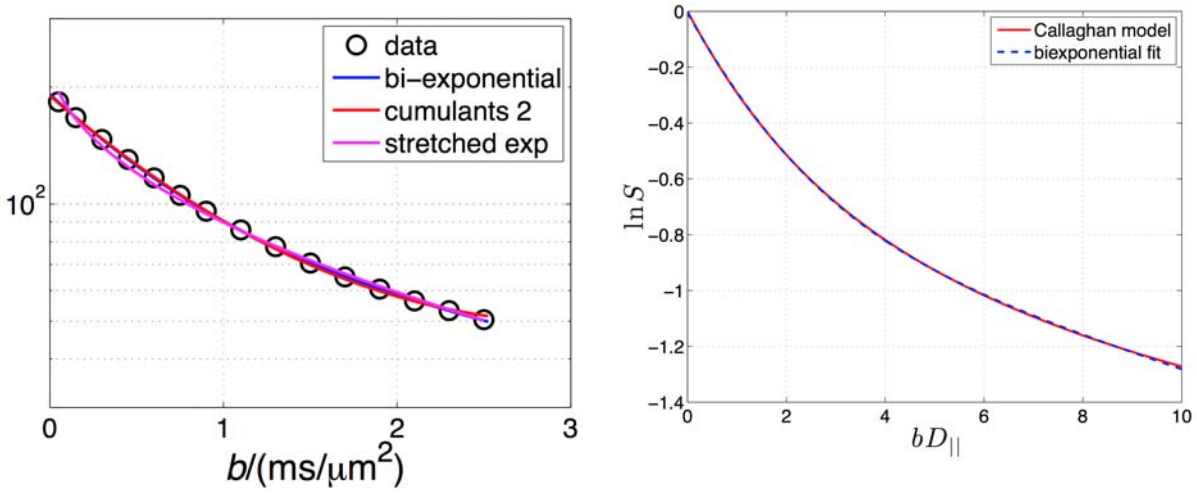

Figure 6: Left: Whole-brain averaged diffusion-weighted signal in a human subject (symbols) as a function of the b-factor. Lines show fitting these data with the bi-exponential model $S = w_1 e^{-bD_1} + w_2 e^{-bD_2}$, the cumulant expansion terminated after the second term $S = e^{c_0 - bD + K(bD)^2/6}$ and the stretched exponential model $S = S_0 e^{-(bD)^\nu}$. Right: Analytical result for the Callaghan model of diffusion in randomly isotropically oriented one-dimensional channels with a diffusivity $D_{||}$ [25] (red line). The signal in this model $S \sim (bD_{||})^{-1/2}$ for $bD_{||} \gg 1$. In spite of this non-exponential behavior, the signal is well fitted by the bi-exponential model.

by molecular motions and, thus, is sensitive to the local (angstrom scale) chemical environment. Changes in this local chemical environment that occur over the mesoscopic scale is a feature that is used in MRI. The fact that longitudinal relaxation is immune to mesoscopic scale modulation of the magnetic field makes it less sensitive to the cellular structure. This reduced sensitivity can be advantageous in enabling a simple interpretation of experimental data. Such an approach is used for evaluation of the capillary permeability in tissues with extravasation of contrast agent (DCE MRI) [21, 22, 23].

7 Data fitting and solution to inverse problems

It is common to validate biophysical models by fitting to experimental data. As mentioned in the context of chemical exchange models, a good fitting quality can be misleading. It does not necessarily validate the model. Examples of successful fitting of different models to the same data are shown in Fig. 6; a comparative analysis of two of the addressed models was presented in Ref. [24].

Low-residual mapping of different biophysical models onto the same data is a manifestation of the ill-posed nature of the inverse problem that underlies the tissue structure determination challenge using MRI. It is one of many problems on the way to the goal that inspires more and more researchers today. Progress made on this challenge is presented in lectures given within this course.

8 Summary

- The MRI signal in biological samples is formed on three distinct length and time scales characteristic of molecules (∼angstroms, picoseconds), cells (∼micrometers, milliseconds), and imaging voxels (∼millimeters, minutes).
- Theoretical models describing the underlying biophysics governing the MR signal formation are a constituent part of probing biological tissue structure (and function) with MRI.
- Diffusion provides a motor for tissue exploration on the cellular scale by MR-reporting molecules.
- Both diffusion and transverse relaxation phenomena are sensitive to the cellular structure, but the potential signatures of many structural features are averaged out due to the macroscopic resolution of MRI. It is necessary to realize what properties survive this averaging.
- Chemical exchange and longitudinal relaxation are less sensitive to structural details, which may be advantageous for data interpretation depending on the measurements goal.
- Chemical exchange is not equivalent to diffusion.
- Good quality of fitting experimental data is a necessary, but not sufficient condition of model validity.

References

[1] Valerij G Kiselev. Transverse relaxation effect of MRI contrast agents: a crucial issue for quantitative measurements of cerebral perfusion. *J Magn Reson Imaging*, 22(6):693–6, Dec 2005.

[2] P. P. Mitra, P. N. Sen, and L. M. Schwartz. Short-time behaviour of the diffusion coefficient as a geometrical probe of porous media. *Phys. Rev. B*, 47 (14):8565–8574, 1993.

[3] Dmitry S. Novikov, Els Fieremans, Jens H. Jensen, and Joseph A. Helpern. Characterizing microstructure of living tissues with time-dependent diffusion, http://arxiv.org/abs/1210.3014, 2012.

[4] Derek K Jones, editor. *Diffusion MRI: Theory, Methods and Applications*. Oxford University Press, 2010.

[5] Yaniv Assaf, Tamar Blumenfeld-Katzir, Yossi Yovel, and Peter J Basser. AxCaliber: a method for measuring axon diameter distribution from diffusion MRI. *Magn Reson Med*, 59(6):1347–1354, Jun 2008.

[6] Daniel Barazany, Peter J Basser, and Yaniv Assaf. In vivo measurement of axon diameter distribution in the corpus callosum of rat brain. *Brain*, 132(Pt 5):1210–20, May 2009.

[7] M. D. Does, E. C. Parsons, and J. C. Gore. Oscillating gradient measurements of water diffusion in normal and globally ischemic rat brain. *Magn. Reson. Med.*, 49:206–215, 2003.

[8] Dmitri B Chklovskii, Thomas Schikorski, and Charles F Stevens. Wiring optimization in cortical circuits. *Neuron*, 34(3):341–7, Apr 2002.

[9] Marco Reisert, Irina Mader, Constantin Anastasopoulos, Matthias Weigel, Susanne Schnell, and Valerij Kiselev. Global fiber reconstruction becomes practical. *Neuroimage*, 54(2):955–62, Jan 2011.

[10] Laura-Adela Harsan, Csaba Dávid, Marco Reisert, Susanne Schnell, Jürgen Hennig, Dominik von Elverfeldt, and Jochen F Staiger. Mapping remodeling of thalamocortical projections in the living reeler mouse brain by diffusion tractography. *Proc Natl Acad Sci U S A*, 110(19):E1797–806, May 2013.

[11] L. Østergaard, R. M. Weisskoff, D. A. Chesler, C Gyldensted, and B. R. Rosen. High resolution measurement of cerebral blood flow using intravascular tracer bolus passages. Part I: Mathematical approach and statistical analysis. *Magn Reson Med*, 36(5):715–25, Nov 1996.

[12] L. Østergaard, A. G. Sorensen, Kwong K. K., R. M. Weisskoff, C Gyldensted, and B. R. Rosen. High resolution measurement of cerebral blood flow using intravascular tracer bolus passages. Part II. experimental comparison and preliminary results. *Magn Reson Med*, 36:726–735, 1996.

[13] J. Dennie, JB Mandeville, JL Boxerman, SD Packard, BR Rosen, and RM Weisskoff. NMR imaging of changes in vascular morphology due to tumor angiogenesis. *Magn Reson Med*, 40:793–799, 1998.

[14] I. Troprès, S. Grimault, A. Vaeth, E. Grillon, C. Julien, J. Payen, L. Lamalle, and M. Décorps. Vessel size imaging. *Magn Reson Med*, 45:397–408, 2001.

[15] Valerij G. Kiselev, Ralph Strecker, Sargon Ziyeh, Oliver Speck, and Jürgen Hennig. Vessel size imaging in humans. *Magn Reson Med*, 53(3):553–63, Mar 2005.

[16] J. L. Boxerman, L. M. Hamberg, B. R. Rosen, and R. M. Weisskoff. MR contrast due to intravascular magnetic susceptibility perturbations. *Magn Reson Med*, 34(4):555–566, Oct 1995.

[17] D. A. Yablonskiy and E. M. Haacke. Theory of NMR signal behavior in magnetically inhomogeneous tissues: The static dephasing regime. *Magn Reson Med*, 32(6):749–763, Dec 1994.

[18] V. G. Kiselev and S. Posse. Analytical theory of susceptibility induced NMR signal Dephasing in a Cerebrovascular Network. *Physical Review Letters*, 81:5696 – 5699, 1998.

[19] V. G. Kiselev and S. Posse. Analytical model of susceptibility-induced MR signal dephasing: Effect of diffusion in a microvascular network. *Magn Reson Med*, 41:499–509, 1999.

[20] Els Fieremans, Dmitry S Novikov, Jens H Jensen, and Joseph A Helpern. Monte carlo study of a two-compartment exchange model of diffusion. *NMR Biomed*, 23(7):711–24, Aug 2010.

[21] G J Parker and P S Tofts. Pharmacokinetic analysis of neoplasms using contrast-enhanced dynamic magnetic resonance imaging. *Top Magn Reson Imaging*, 10(2):130–42, Apr 1999.

[22] P S Tofts, G Brix, D L Buckley, J L Evelhoch, E Henderson, M V Knopp, H B Larsson, T Y Lee, N A Mayr, G J Parker, R E Port, J Taylor, and R M Weisskoff. Estimating kinetic parameters from dynamic contrast-enhanced T(1)-weighted MRI of a diffusable tracer: standardized quantities and symbols. *J Magn Reson Imaging*, 10(3):223–32, Sep 1999.

[23] J S Taylor, P S Tofts, R Port, J L Evelhoch, M Knopp, W E Reddick, V M Runge, and N Mayr. MR imaging of tumor microcirculation: promise for the new millennium. *J Magn Reson Imaging*, 10(6):903–7, Dec 1999.

[24] Valerij G Kiselev and Kamil A Il'yasov. Is the "biexponential diffusion" biexponential? *Magn Reson Med*, 57(3):464–9, Mar 2007.

[25] P. T. Callaghan, K. W. Jolley, and J. Lelievre. Diffusion of water in the endosperm tissue of wheat grains as studied by pulsed field gradient nuclear magnetic resonance. *Biophys J*, 28:133–141, 1979.